Two-dimensional magnetic colloids under shear

Supplementary Information

Tomaž Mohorič,[1,2] Jure Dobnikar,[1] and Jürgen Horbach[3]

[1]*International Research Centre for Soft Matter, Beijing University of Chemical Technology, Beijing 100029, P.R. China*

[2]*Faculty of Chemistry and Chemical Technology, University of Ljubljana, Večna pot 113, 1000 Ljubljana, Slovenia*

[3]*Institute for Theoretical Physics II: Soft Matter, Heinrich-Heine-Universität Düsseldorf, 40225 Düsseldorf, Germany*

I. BONDING PATTERNS IN DEFORMED GEL

Bonding patterns in a gel (at the opening angle $\theta = 48°$) are more quantitatively characterized on Figure S1. We define two colloids as bonded if their interparticle distance is less than 1.2σ.

First, on Figure S1**A** we present bonding probability distribution P_n, i.e. probability that a colloid forms exactly n bonds, for the unsheared system ($\dot{\gamma} = 0$). As could be deduced from the snapshots (see Figure 3 in the main text), most of the particles form 2 or 3 bonds and there is also non–negligible fraction of non–bonded particles.

Figure S1**B** shows changes in the bonding distribution, ΔP_n, at different strains for the lowest (black dashes) and the highest (red crosses) shear rate. Left part of the figure presents ΔP_n for the system's bulk ($y \approx 0$) and right part for the boundaries ($y \approx \pm L/2$). For the highest $\dot{\gamma}$ there are hardly any changes in bulk P_n. On the other hand at the boundaries, there are significant changes in P_n already at $\gamma = 0.1$, where the fraction of single–bonded particles ($n = 1$, free ends of chains) increases on the account of three–bonded "bridges" ($n = 3$). Initially, after the shear is applied, these "bridges" are the weak–points, where the bond breakage mainly occurs. In later stages, non–bonded particles ($n = 0$) incorporate into the network, as suggested by the drop in P_0 and increase in P_2. For the lowest shear rate ΔP_n for the bulk and boundary look very similar. A fraction of non–bonded particles ($n = 0$) incorporates into the network, which results in an increase of three- ($n = 3$) and four–bonded ($n = 4$) particles. At $\gamma = 10$ almost all non–bonded particles are incorporated into the network. However, in the bulk this results in almost equal increase of P_2, P_3 and P_4, while at the boundaries only P_2 increases.

To determine average bond orientation we calculated bonding anisotropy, defined as $\varepsilon_{\text{bond}} = \langle u_{\text{y}}^2 \rangle / \langle u_{\text{x}}^2 \rangle$. Here u_{x} and u_{y} are x and y–component of the unit vector connecting centers of two bonded particles. Note that for a uniformly distributed bond orientation bonding anisotropy is 1. $\varepsilon_{\text{bond}}$ as a function of coordinate y at different strains for the lowest (black circles) and the highest (red squares) shear rate is presented on Figure S1**C**. At $\gamma = 0.1$ (top row) bonding anisotropy equals 1 independently of the shear rate. At $\gamma = 1$, when stress reaches the maximum for $\dot{\gamma} = 10^{-5}$, bonding anisotropy is about 0.8 and uniformly distributed. This clearly shows the tendency of the network to align its bonds with direction of the applied shear. With a further increase in strain, deviation from an isotropic bond orientation becomes even more pronounced. On the other hand, for the highest $\dot{\gamma}$ only bonds at the boundaries ($y \approx \pm L/2$), where shear is applied, tend to align with the shearing field.

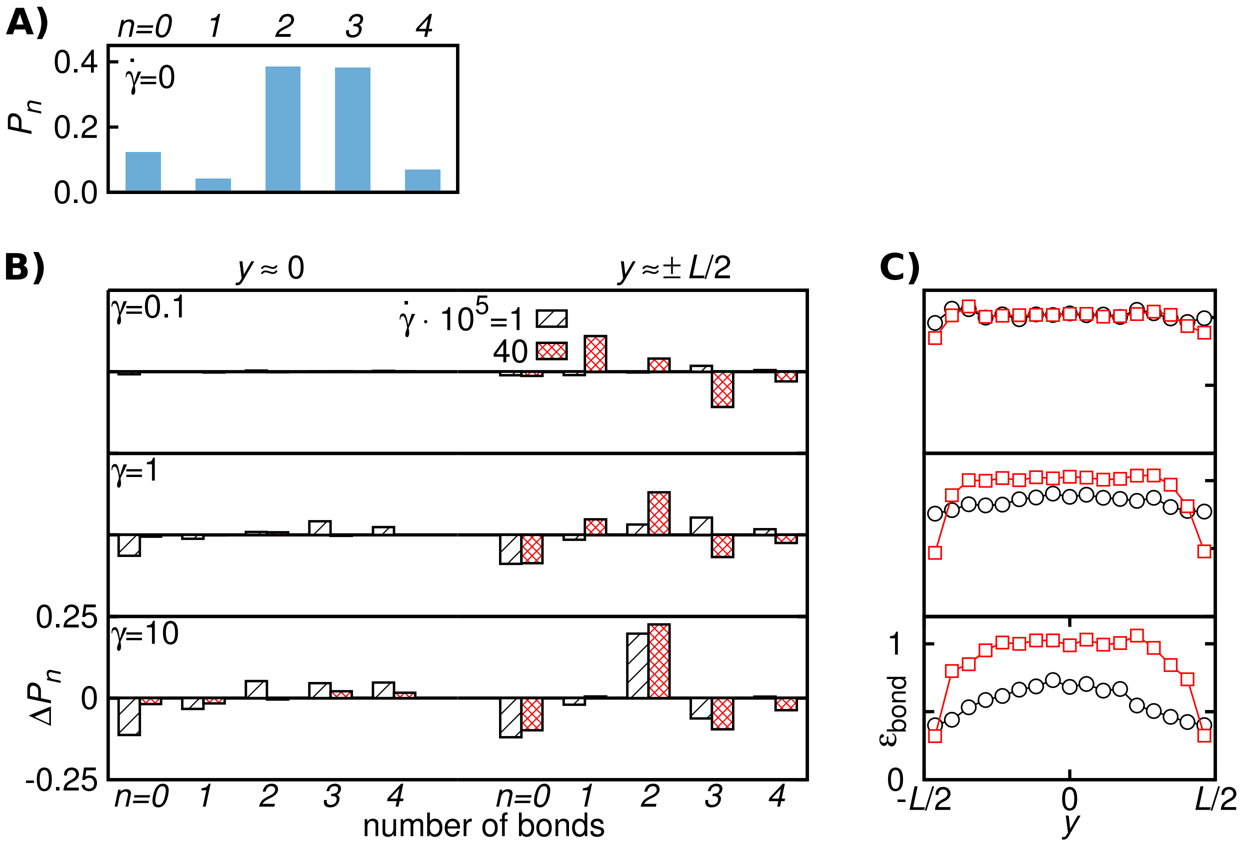

FIG. S1. **A)** Bonding distribution, P_n, for the unsheared network ($\dot{\gamma} = 0$) for the case of the opening angle $\theta = 48°$. **B)** Changes in bonding distribution, ΔP_n, at strain γ=0.1 (top row), 1 (middle row), and 10 (bottom row) for the lowest (black) and the highest (red) shear rate $\dot{\gamma}$. The left half presents ΔP_n in the center of simulation box ($y \approx 0$), while the right half shows the same but for the borders ($y \approx \pm L/2$). **C)** Bonding anisotropy $\varepsilon_{\text{bond}}$ as a function of y at strain γ=0.1 (top row), 1 (middle row), and 10 (bottom row) for the lowest (black circles) and the highest (red squares) shear rate $\dot{\gamma}$.

II. GEL RELAXATION AFTER SWITCHING OFF THE SHEAR

To further investigate the stability of deformed gel structures ($\dot{\gamma} = 10^{-5}$), we switched off the shear at various points in stress–strain curves and monitored the subsequent relaxation of stress. Figure S2 (left) shows the stress–time relation after switching off the shear at strain values $\gamma = 0.1$ (black), 1 (blue), 10 (green) and 30 (red). In all the cases the stress decreases somewhat towards $\sigma_{\mathrm{xy}} = 0$. Surprisingly, even for the relaxation from $\gamma = 0.1$, where shear–induced structural changes are relatively small, σ_{xy} remains almost unchanged. Accordingly, only minor structural changes are observed. This suggests that the gel structure at every point in the stress–strain curve is effectively trapped in a deep local energy minimum. By increasing the reduced temperature T^* by a factor of 10 (which would correspond to decreasing the external field in experiment from $B_0 \approx 10$ mT to $B_0 \approx 3$ mT) we effectively decreased the energetic barriers. Stress–time relations at these conditions are plotted on Figure S2 (right). Stress relaxation towards its equilibrium value ($\sigma_{\mathrm{xy}} = 0$) is much more complete at elevated temperature. Hence, the ability of the system to store a given stress decreases with temperature.

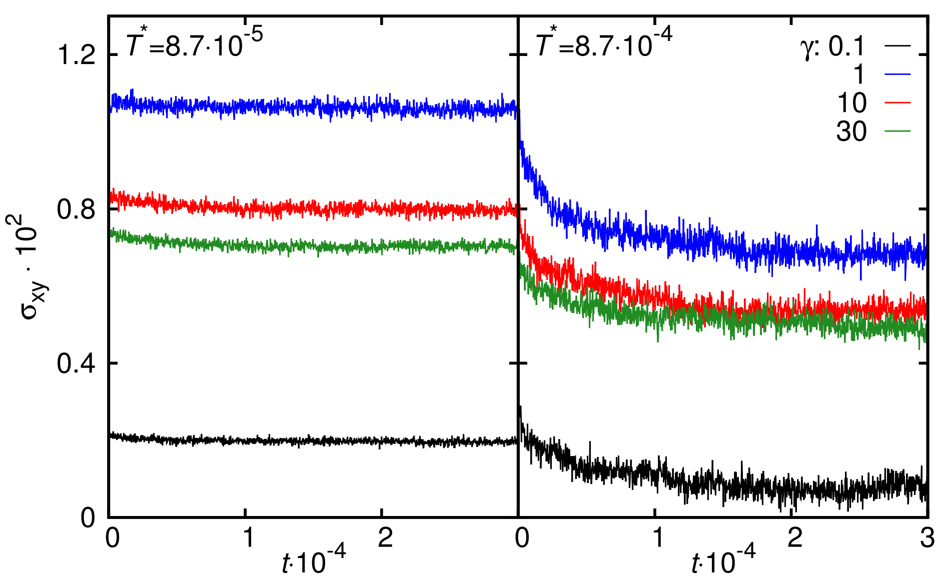

FIG. S2. Stress–time relation after switching off the shear at different strains γ (colors) and at temperatures $T^* = 8.7 \cdot 10^{-5}$ (left) and $T^* = 8.7 \cdot 10^{-4}$ (right).

III. MOVIES OF FULL TRAJECTORIES

We have prepared movies of trajectories and corresponding stress–strain curves in the form of `.gif` files for the lowest and the highest shear rate $\dot{\gamma}$ at each opening angle θ. The name of the file is composed from values of the opening angle and the shear rate.

Particles in the simulated cell are depicted with dark–gray color, while periodic images in y–direction are shown in light–gray. For the opening angle $\theta = 0°$ also 5 and 7–fold disclinations are shown with blue and red.

List of files:

- `theta_0_shear_0.00001.gif`
- `theta_0_shear_0.0004.gif`
- `theta_48_shear_0.00001.gif`
- `theta_48_shear_0.0004.gif`
- `theta_50_shear_0.00001.gif`
- `theta_50_shear_0.0004.gif`